Signal Processing for Photoacoustic Tomography

V. Moock*, C. García-Segundo†, E. Garduño‡, F. Arámbula Cosio,†
J. Jithin§, P. van Es§, S. Manohar§ and W. Steenbergen§

*Posgrado en Ciencia e Ingeniería de la Computación, Universidad Nacional Autónoma de México (UNAM)
Ciudad Universitaria, C.P. 04510, México, D. F., Email: verena.moock@ccadet.unam.mx

†Centro de Ciencias Aplicadas y Desarrollo Tecnológico, UNAM, Circuito Exterior, Apdo. Postal 70-186
‡Instituto de Investigaciones en Matemáticas Aplicadas y en Sistemas, UNAM, Circuito Escolar, Apdo. Postal 20-726
§Biomedical Photonic Imaging Group, MIRA Institute, University of Twente, P.O. Box 217, NL-7500 AE Enschede

***Abstract*—This study examines one of the open problems yet to solve in photoacoustic tomography: How to prepare photoacoustic signals to ensure interpretation as projection data? The main part of this difficulty is related to the setting of the linear photoacoustic transport model. Notably errors are due to the discrepancy between the mathematical reconstruction and the physical realization: Tomographic image reconstruction from projections require a linear acquisition system. However in practice, the physical reality presents different non-linear phenomena. In account of this incompatibility, it was our purpose to provide some advancement in signal processing for dealing the projection issue while considering different perspectives in the interpretation of the transport model to be applied in a broader manner. Numerical examples are analyzed in detail and unveil the foundations for photoacoustic signal processing methodologies focused on the task of tomographic image reconstruction from projections.**

***Index Terms*—Signal processing techniques for acoustic inverse problems; remote sensing methods, acoustic tomography; ultrasonographic imaging.**

PACS numbers: 43.60.Pt; 43.60.Rw; 87.63.dh.

I. Introduction

In the last decade the development of photoacoustic imaging methods has increased, particularly because it is a promising tool for early non-invasive and non-ionizing detection of breast cancer. Photoacoustic images uniquely combine electromagnetic (EM) and ultrasonic (US) information about (biological) objects, e.g. human breast tissue. The operation principle specifies that the object be exposed to infrared radiation with laser pulses, thereby inducing the photoacoustic effect: The absorption of light, while dissipating in a non-radiative manner, produces mechanical disturbances expressed as changes in the pressure distribution. This distribution is confined in time and space and is expressed as a mechanical impulse that is recorded by specific detectors [1] outside the region of interest. Once photoacoustic data is captured, the required projection information therein, in correspondence to the transport model, is deduced via signal processing techniques. Certainly, the common usage of a homogeneous plane wave transport model for photoacoustic applications, as outlined by Wang et al. in [13], is over-simplified for most biomedical applications. This is in view of assumptions on homogeneous media and negligible influence of viscosity and diffusion. In fact, these assumptions breakdown when imaging real biological tissue such as breasts and corrections have to be incorporated into the model. For instance, posterior sound velocity corrections have to be involved in image processing algorithms, as shown in [7]. Consequently, we need a better analytical description of the photoacoustic transport to reconstruct high-quality images and take effective advantage of the US resolution and EM contrast present in this imaging modality. Notwithstanding, for computed tomography (CT) it is technically unavoidable to approximate registered signals as linear projection data; in accordance with the selected transport model.

This manuscript proposes a method that takes into account viscous and scattering media properties for a linear transport model. Departing from these considerations, our contribution which is partitioned as follows: In section II we describe image reconstruction as an inverse source problem with the aim of identifying the role of the linear transport operator and recall the necessary boundary conditions. Then, in section III we present a new classification of the different linear wave forms with diffraction patterns; these will bring us closer to a more realistic transport description, whenever in practice more precise model conditions can be set up *a priori*. The main section of this study is dedicated to the photoacoustic signal processing methodologies that outline the key part to combine mathematical reconstruction and physical realization. Based on the understanding that reconstruction principles are governed by the same rules that are followed in the US-CT and photon detection from projections, in section V we review the CT strategies designed for modalities with diffraction. The literature in the field of photoacoustic methods mainly utilize backprojection strategies; despite, there are several other tomographic methods; whence reconstruction can be done using many different algorithms. Next we analyze several of these methods, with the aim of determining possibly more efficient reconstruction techniques for photoacoustic imaging.

978-1-4673-0964-6/12/$31.00 ©2012 IEEE

II. Inverse source problem

The photoacoustic image reconstruction can be considered as an inverse source problem in the sense that the initial pressure distribution $f(\mathbf{x}) = \psi(\mathbf{x}, 0)$ acts as the source; this is provided by electromagnetic absorption, where $\psi : \mathbb{R}^n \times \mathbb{R}_+ \quad \mathbb{R}$ and $n \leq 3$ is the spatial dimension. The propagation of this pressure distribution in a linear model allows a description as a homogeneous wave equation in terms of a linear differential operator $\mathcal{L}$ of second order with (temporal gradient) initial conditions,

$$\begin{aligned} \mathcal{L}\psi(\mathbf{x}, t) &= 0 && (1)\\ \psi(\mathbf{x}, 0) &= f(\mathbf{x}) && (2)\\ \partial_t\psi(\mathbf{x}, 0) &= 0. && (3) \end{aligned}$$

This is applied to photoacoustic imaging, under the assumption that there exists a trace of the forward problem (1-3) that is in correspondence with the ultrasonic sensor registering at the boundary of the observed region Ω,

$$\psi(\overline{\mathbf{x}}, t) = g(t), \qquad \overline{\mathbf{x}} \quad \partial\Omega. \tag{4}$$

Given the photoacoustic signal $g(t)$ as a damped wave in a possibly inhomogeneous environment, one can make inferences on the constituent terms of the wave equation. The simplest and most used description in accordance with [13] is given by the operator d'Alembert $\Box$ acting on the pressure distribution $\psi(\mathbf{x}, t)$; variable in space and time,

$$\mathcal{L}_1\psi(\mathbf{x}, t) := (\partial_t^2 - \mathbf{c}^2 \quad ^2)\psi(\mathbf{x}, t) =: \Box\psi(\mathbf{x}, t), \tag{5}$$

where ∂_t^2 represents the second temporal derivative. Accordingly $\quad ^2$ is the Laplace operator and $\mathbf{c}^2$ is a measure of the sound speed. On applying the principle of Duhamel, the inverse problem in (1-3), to derive the image data $f(\mathbf{x})$, appears as its equivalent version in terms of the following inhomogeneous wave equation (see [10]),

$$\begin{aligned} \mathcal{L}\psi(\mathbf{x}, t) &= f(\mathbf{x})\partial_t\delta(t), && (6)\\ \partial_t\psi(\mathbf{x}, 0) &= 0, && (7)\\ \psi(\mathbf{x}, t_-) &= 0, \qquad t_- < 0. && (8) \end{aligned}$$

Here, δ represents the temporal delta function related to the illumination. For a physically homogeneous medium, the forward solution of the above problem expressed by the operator $\Box$ in dimension n turns out to be specified in terms of the spherical Radon transform

$$\psi(\overline{\mathbf{x}}, t) = g(t) \sim \mathcal{R}_\circ[f](t). \tag{9}$$

Since the spherical Radon transform has its known inverse operator, analyzed in [5], the inverse problem gets solved. The image data can be reconstructed numerically if sufficiently measurements of the homogeneously illuminated object of interest are taken. Notwithstanding, in practice the inverse problem is ill-conditioned. A physically acceptable, approximate, solution can only be obtained, when *a priori* information is taken into account, satisfying additional constrains, considering instrumental aspects of the acquisition system, as described in [2].

III. Generalization of the transport model

For miscellaneous biomedical applications of photoacoustic imaging it is of interest to achieve a more appropriate linear model of the underlying transport than what the operator $\Box$ fulfills; which can include for example viscous and/or scattering media properties. In order to maintain a second order linear model for tomographic reconstructions we present the following extensions:

$$\begin{aligned} \mathcal{L}_1 &:= \Box, && (10)\\ \mathcal{L}_2 &:= \Box + \ \mathbf{v}, \quad , && (11)\\ \mathcal{L}_3 &:= \Box + d, && (12)\\ \mathcal{L}_4 &:= \Box + \ \mathbf{v}, \quad + d. && (13) \end{aligned}$$

The literature focused on the photoacoustic transport problem exhibits that the first instance (10) for plane waves and frequently appears in systems assumed as physically homogeneous. The Boltzmann operator[1] (11) involves a constant $\mathbf{v}$, allowing wave attenuation as a first approximation to the presence of viscosity in the referred system. The Helmholtz operator (12) in turn involves a constant d, accepting wave augmentation as a first approximation for the presence of linear diffusion in the system under study. Both additional contributions are present in the fourth operator[2], related to the Heaviside telegraph equation (13). The latter model symbolizes the most general second order linear photoacoustic transport and is analyzed for the purpose of image reconstruction in [12]. Although, the choice of the above operators will not alter the signal processing routines below, it will somewhat vary the reconstruction conditions.

IV. Photoacoustic signal processing

Photoacoustic signals can be captured by ultrasonic detectors as a time sequence of voltage variations. Figure 1 shows a one-dimensional scan of a sample with two small inhomogeneities over the interval $[0, t_1]$, $t_1 = 72$ μs, at a sample frequency of 80 MHz.

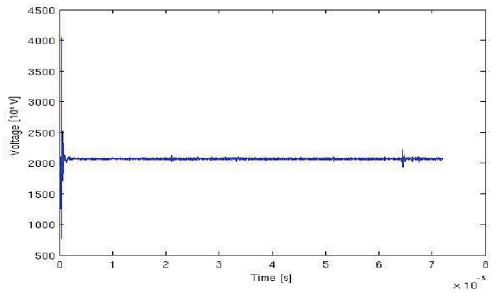

Fig. 1: **D**: Raw data captured by an US detector.

[1]To the best of our knowledge, physical models for photoacoustic and photothermal applications by the presence of continuous conditions present only one of two terms, $\mathbf{v_x}$ o v_t:
$\Box + \langle \mathbf{v_x}, \nabla \rangle \overset{\text{cont.}}{\equiv} \Box + v_t\partial_t$.

[2]Possibly there is an equivalence relation:
$\Box + \langle \mathbf{v_x}, \nabla \rangle + d \overset{\text{cont.}}{\equiv} \Box + v_t\partial_t + d$.

In order to improve the low signal-to-noise ratio (SNR) of the photoacoustic raw data is necessary to make some preprocessing. It is already known that the dominant initial peak is related to the voltage source and the direct impact of momentum on the sensor [4]. Since there is little contribution to the photoacoustic information of the region of interest within the time interval $[0, t_0]$, $t_0 = 2.0$ μs this part was ignored for further processing. Linear trends in the carrier signal were also removed and normalized with respect to atmospheric pressure $p_0 \approx 2.0$mV. For this case study auto-correlation was considered as a useful global technique to improve the SNR; see the result of preprocessing in Figure 2.

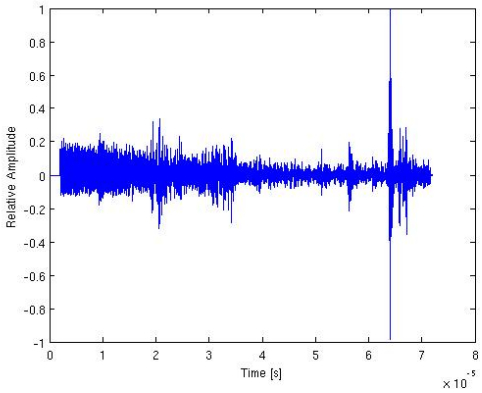

Fig. 2: $\mathbf{D}_0$: Calibration by suppressing the influence of the instrumentation device and auto-correlation.

The photoacoustic image data are provided by the detector response and become readily accessible for reconstruction after using a global signal processing techniques; miscellaneous are described next:

1) Calculating the envelope function env(t) as in [11],

$$\mathrm{env}(\mathbf{D}_0) = \mathbf{D}_0 - i\mathcal{H}(\mathbf{D}_0)\,, \tag{14}$$

with respect to the normalized data $\mathbf{D}_0 = \mathbf{D} - p_0$ and the Hilbert transform $\mathcal{H}$, applied to the test data in Figure 3.

2) Calculating the statistical measure of the amplitude variation of the photoacoustic pressure, indicated by the effective sound pressure eff(t), which is equal to the root mean square (RMS) of the normalized signal $\mathbf{D}_0$,

$$\mathrm{eff}(\mathbf{D}_0) = \sqrt{\frac{\sum_{t_+=-\ v/2}^{v/2} \mathbf{D}_0^2(t+t_+)}{v}}, \tag{15}$$

where the size of the reference window v, considered when calculating RMS, is set to 21 in the numerical example presented in Figure 4.

3) Rectification of the measured signal [3]: Half wave as well as full wave rectification may be chosen to point out the absolute pressure distribution, see Figure 5.

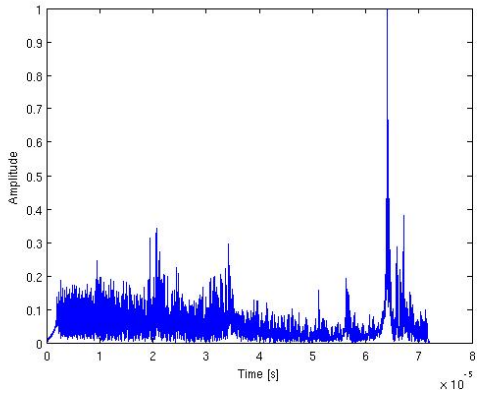

Fig. 3: $\mathbf{D}_0^+ = \mathrm{env}(\mathbf{D}_0)$: Normalized envelope function.

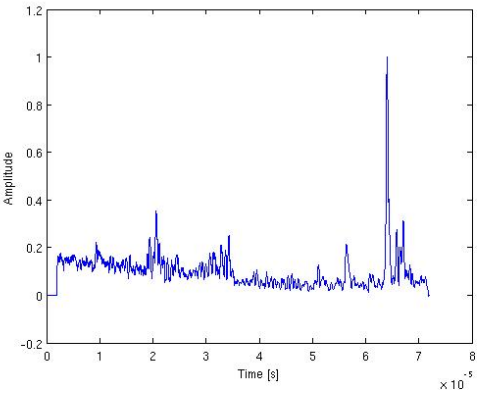

Fig. 4: $\mathbf{D}_0^+ = \mathrm{eff}(\mathbf{D}_0)$: Normalized effective pressure.

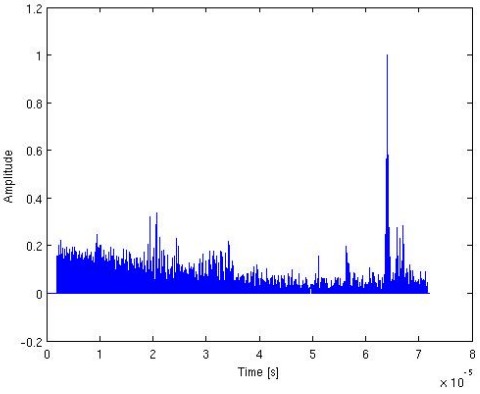

Fig. 5: $\mathbf{D}_0^+$: Normalized half wave rectification.

After successfully applying one of the above filtering methodology, the processed data $\mathbf{D}_0^+$ was further enhanced by thresholding in relation to the estimated value of the SNR. The signal was additionally cleared by convolution with the ideal impulse function, particularly with regard to secondary sampling to carry out the requested image resolution. When all mentioned signal processing is performed, a set that approximates the data g is supplied for finally solving the inverse problem.

V. Tomographic image reconstruction

The fundamentals of computerized tomography are based on the reconstruction from projections. Given the photoacoustic data, the geometry settings for the tomographic reconstruction algorithm have to be in accordance with the projection concept within the photoacoustic model. Consequently, the transport model is restricted to a linear system. Yet, the physical reality may not fulfill the linearity condition. Hence, digital processing routines would be needed to linearize the data for reconstruction purposes.

Once processing true projection data, computerized tomography offers a multitude of reconstruction algorithms. All tomographic methods for images reconstruction can be classified into two groups according to [6]:

(A) Transform-based methods and
(B) Series expansion methods.

These groups particularly differ in the mathematical model of their specification. Transform-based methods are very efficient and fast in operating time. Besides, for linear projections, these algorithms are exact if the system is noise-free. The most intuitive and less complex algorithm is the backprojection routine. Unfortunately, small errors have severe influence on reconstruction results: multiple artifacts in the reconstructed image make a digital biopsy impossible. On the other hand, series expansion methods, mainly typified by ART, also produce exact solutions for the absence of noise. These methods consume more computational resources, but are not restricted to linear models. Corrections to the projection approach can be considered iteratively.

In the following subsections, we show results of implementations of representative algorithms of both families for photoacoustic methods. An adequate phantom for the case study was made of agar where inhomogeneities have been introduced. These local inhomogeneities of different concentrations allow interpretations as tumor propagations. The colorized schema in Figure 6 illustrates the geometric parameters of the experimental setup with a passive element as a primary US source, carried out by [7]. The intention of this figure is also to provide a clearer idea of how the photoacoustic signals are interpreted.

A. Photoacoustic backprojection

Backprojection algorithms are very important techniques for tomographic image reconstruction. The methodology can be considered as the direct numerical application of the inversion formula for the (spherical) Radon transform. Thus, we discretized in (9) the given photoacoustic signal g received by the detector array to the vector $\mathbf{g}$ and interpret that as the integral of the US waves along the aperture, $\mathcal{R}_\circ \mathbf{f} = \mathbf{g}$ over $L_2(\Omega)$, where $\mathbf{f}$ represents a

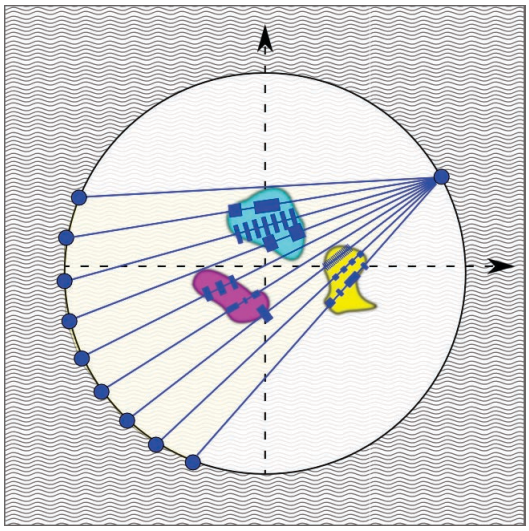

Fig. 6: Phantom, sensor and signal interpretation: high pressure amplitude refers to mayor pressure distribution.

discrete estimate of the image vector. With the aim to get a good approximation, we apply the signal processing as mentioned in section IV and compare their strategies. The reconstruction is performed via iteration over all detector positions and carry out photoacoustic backprojection, very similar to the program for X-rays in [6], but on spherical geometries. The visible cone of each detector element is estimated by the a half-angle of 15° in consideration of [8]. The result with effective pressure signal processing, is shown in Figure 7 for the image resolution of 200×200 pixels. Considerably, the presence of artifacts due to few and erroneous projection data. Justified by the difference between the phantom and test results that, we conclude for backprojection reconstructions from a series of few scans, it is particularly important to implement more accurate or rather corrected signal processing for photoacoustic data.

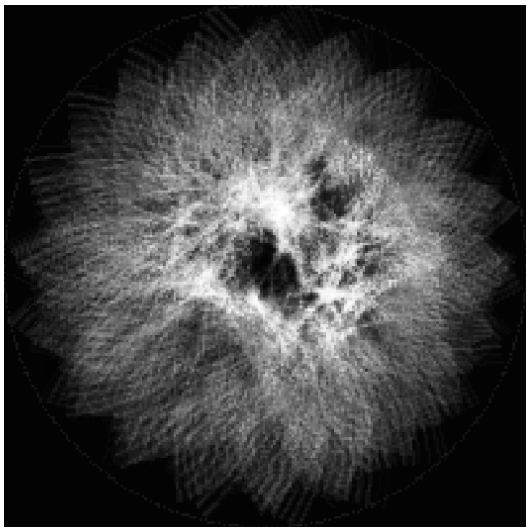

Fig. 7: Examplary photoacoustic backprojection.

B. Photoacoustic ART

ART represents a class of iterative algorithms, not only for image reconstruction from a series of projections, but for solving universal linear systems, and is also known as the Kaczmarz method. In the retrieval of an approximate, physically acceptable solution of the inverse problem ART principally represents a good strategy to attack the ill-posedness of the model. The following notation is consistent with F. Natterer [9], except for changes of letters to be consistent with the previous declaration. Let $A_j f = g_j$ be a system with $A_j : H \quad H_j$ bounded linear operators of Hilbert space H in the Hilbert space H_j, respective to every projection $j = 1, , ..., p$. We resume the model to

$$A = \begin{pmatrix} A_1 \\ \vdots \\ A_p \end{pmatrix}, \quad g = \begin{pmatrix} g_1 \\ \vdots \\ g_p \end{pmatrix}, \qquad Af = g.$$

The orthogonal projection P_j in H on the affine subspace $A_j f = g_j$ is given by $P_j f = f + A_j^*(A_j A_j^*)^{-1}(g_j - A_j f)$. The Kaczmarz procedure with relaxation w (no relaxation if $w = 1$) to solve $Af = g$ is

$$f^{k+1} = P^w f^k, \tag{16}$$

with $P^w = P_p^w ... P_1^w$, $P_j^w = (1 - w)\mathbf{I} + wP_j$. The following describes a step explicitly: set $f^{k,0} = f^k$ to compute $f^{k,j}$ for $j = 1, ..., p$ of according to

$$f^{k,j} = f^{k,j-1} + \omega A_j^*(A_j A_j^*)^{-1}(g_j - A_j f^{k,j-1}) \tag{17}$$

$$= f^{k,j-1} + w\frac{g_j - A_j f^{k,j-1}}{A_j \ ^2} A_j^t, \tag{18}$$

for all $j = 1, ..., p$, and ultimately, we get $f^{k+1} = f^{k,p}$.

The ultimate advantage of ART is its versatility. The method of series expansion is suitable for all scanning geometry and also for problems with incomplete data. ART for $0 < w < 2$ converges to a general solution or to the minimum norm solution of $Af = g$, if the linear system is consistent, see [9]. It should be perceived that $P^w f^k \ < 1$. Unfortunately, we examine that the actual photoacoustic equation system is ill-posed.

VI. Discussion, conclusions and future work

The problem of how to prepare photoacoustic signals to ensure by signal processing interpretation as projection data for tomographic reconstruction was examined. The contemplated digital methodologies unveil foundations for further improvements on image reconstructions. Still, the discrepancy between mathematical conditions and the physical realization is not balanced so far. Certainly, a proper treatment of photoacoustic signals requires more a sophisticated processing. All presented routines are very versatile tools for many different digital treatments; yet many promising denoising strategies for US signals are left to implement (e.g. wavelet analysis).

For the algorithmic task on image reconstruction (from few projections) we still have to stabilize the convergence on our ART reconstruction results, that suffer the ill-posedness of the problem structure. A mathematical acceptable solution of minimal norm will not solve the reconstruction task in the physical sense. Further regularization techniques (e.g. Tikhonov-Phillips) or similar approximation methods supposably will produce better results, as recommended by [9] for CT in general.

Acknowledgments

The authors gratefully acknowledge the Biomedical Photonic Imaging (BMPI) group at the MIRA Institute for Biomedical Technology and Technical Medicine at the University of Twente for the valuable discussions and their assistance with photoacoustic data from the Twente Computer Tomograph system for our analysis. We appreciate the administrative and financial support of the Prosgrado en Ciencias e Ingeniería de la Computación (PCIC) at the Universidad Nacional Autónoma de México (UNAM), of the Consejo Nacional de Ciencia y Tecnología (CONACYT) and of the Instituto de Ciencia y Tecnología del Distrito Federal (ICYT).

References

[1] A. Guadarrama-Santana C. García-Segundo A. García-Valenzuela B. Reyes-Ramirez, J. G. Bermúdez-Servín. 2d-capacitive-pyroelectric sensor array for photoacoustic detection. Symposium of Photothermal Phenomena, SMCTSM 2012.

[2] M. Bertero and P. Boccacci. *Introduction to Inverse Problems in Imaging*. IOP Publishing Ltd, 2nd ed. edition, 2002.

[3] K.S. Boyle and T.C. Tricas. Pulse sound generation, anterior swim bladder buckling and associated muscle activity in the pyramid butterflyfish, hemitaurichthys polylepis. *J. Exp. Bio.*, 213:3881–3893, 2010.

[4] A.J. Smith C. García-Segundo and J.-P. Connerade. Optically induced non-radiative fast pulses in metals. *J. Mod. Opt.*, 20:233–253, 2004.

[5] S.K. Patch D. Finch and Rakesh. Determining a function from its mean values over a family of spheres. *SIAM J. Math. Anal.*, 35:1213–1240, 2004.

[6] G.T. Herman. *Fundamentals Of Computerized Tomography - Image Reconstruction From Projections*. Advances In Computer Vision And Pattern Recognition. 2nd ed. edition, 2010.

[7] S. Resink-D. Piras J. van Hespen C. Slump W. Steenbergen-T. van Leeuwen J. Jose, R. Willemink and S. Manohar. Passive element enriched photoacoustic computed tomography for simultaneous imaging of acoustic propagation properties and light absorption. *Opt. Express*, pages 2093–2104, 2010.

[8] D.H. Johnson and D.E. Dudgeon. *Array Signal Processing, Concepts And Techniques*. Prentice Hall Signal Processing Series. 1993.

[9] F. Natterer and F. Wübbeling. *Mathematical Methods In Image Reconstruction*. Monographs on Mathematical Modeling and Computation. SIAM, 2001.

[10] H. Grün M. Haltmeier P. Burgholzer, J. Bauer-Marschallinger and G. Paltauf. Temporal back-projection algorithms for photoacoustic tomography with integrating line detectors. *Inverse Problems*, 23:S65–S80, 2007.

[11] T.O. Müller R. Liu R. Stotzka, N.V. Ruiter and H. Gemmeke. High resolution image reconstruction in ultrasound computer tomography using deconvolution. *SPIE Med. Imaging*, 2005.

[12] E. Garduño V. Moock, C. García-Segundo and F. Arámbula Cosio. Classification of diffusion transport models for reconstruction from projections. In preparation for submission.

[13] M. Xu and L.V. Wang. Photoacoustic imaging in biomedicine. *Review of Scientific Instruments*, 66:1–20, 2006.